Journal of Controlled Release, 24 (1993) 27–44

Application of supercritical fluids for the production of sustained delivery devices

Pablo G. Debenedetti, Jean W. Tom, Sang-Do Yeo, Gio-Bin Lim[1]

Department of Chemical Engineering, Princeton University, Princeton, NJ 08544, USA

(Received April 1992; accepted in revised form 21 July 1992)

Supercritical fluids are attractive as vehicles for the formation of particles of biomedical interest. We review two novel techniques: the rapid expansion of supercritical solutions for the formation of solvent-free, drug-loaded, injectable microspheres, and the gas anti-solvent precipitation process for the formation of ultrafine and biologically active protein powders.

Key words: Supercritical fluid; Sustained delivery device; Rapid expansion; Anti-solvent precipitation

Introduction

Supercritical fluids offer considerable promise as vehicles for the formation of particles of biomedical interest. Two techniques have been used to date. In one, particles are formed as a result of the rapid expansion of a supercritical fluid. In the other, the supercritical fluid is used as an anti-solvent that causes particle precipitation from a liquid solution. The former process is known as rapid expansion of supercritical solutions (RESS; [1]); it is of interest as an alternative to conventional size-reduction methods [2–4], and a novel route to solvent-free drug-loaded microspheres [5–6]. The second method is known as gas anti-solvent precipitation (GAS; [7]; it is of interest in the formation of fine peptide and protein powders [6,8].

Correspondence to: Pablo G. Debenedetti, Department of Chemical Engineering, Princeton University, Princeton, NJ 08544, USA.

[1]Current address: Department of Chemical Engineering, University of Suwon, P.O. Box 77, Suwon, Korea 440-660.

RESS is an attractive alternative to conventional methods for the production of drug-loaded polymeric microspheres since it requires no surfactants, yields a solvent-free product (the solvent is a dilute gas after expansion), and allows processing at moderate temperatures. In conventional precipitation methods (such as solvent–anti-solvent and solvent evaporation), organic solvents, surfactants, and suspending agents are required, and must be removed from the microspheres before their use in vivo. Alternative techniques, such as spray drying and melt-pressing followed by grinding, involve heat, which may affect the drug's stability, and multiple processing steps. In contrast, the coprecipitation of bioerodible polymers and drugs by RESS can, in principle, produce drug-loaded microspheres in a single processing step, avoiding the use of liquid organic solvents, surfactants, and heat (if low-critical-temperature solvents are used).

The application of the GAS process to the formation of microparticulate protein powders is a very recent development [6,8]. Controlled release systems for peptides and proteins offer sev-

sure by factors of up to 10^6. Furthermore, the decompression of a supercritical fluid containing dissolved substances can be accomplished very rapidly ($\leq 10^{-5}$ s) using nozzles, capillaries, or orifices, and constitutes a mechanical perturbation which travels at the speed of sound. Consequently, the rapid expansion of supercritical solutions can lead to very high supersaturation ratios. The combination of a rapidly propagating mechanical perturbation and high supersaturation ratios is the distinguishing feature of RESS. The former leads to uniform conditions within the nucleating medium, and hence in principle to narrow particle size distributions; the latter, to small particles. Since the supercritical fluid is an ideal gas after expansion, the solid product is recovered in pure, solvent-free-form.

Historically, the first observation of changes in particle size and morphology upon expansion of supercritical solutions was made by Hannay and Hogarth [19], who characterized precipitated solids as 'snow' in a gas and 'frost' on glass. More than a century elapsed before Krukonis [20] carried out the first modern investigation of RESS, demonstrating the potential of this technique for particle formation, size reduction, and comminution of a wide variety of materials. For a recent review see Tom and Debenedetti [21].

The GAS process

A more recent application of supercritical fluids to particle formation is gas anti-solvent (GAS) precipitation [6–8, 22–24]. Here, a supercritical fluid is used as an anti-solvent that causes precipitation of solids. The solids are first dissolved in a liquid, and a supercritical fluid (having a low solvent power with respect to the solids, but miscible with the liquid) is added to precipitate the solids. The size distribution of the precipitate depends on the rate of addition of the supercritical fluid [7–8]. As shown in Fig. 4, the dissolution of supercritical fluids in liquids is often accompanied by a large volume expansion and, consequently, a reduction in the liquid's solvent power. Rapid addition of a supercritical fluid results in a sudden reduction in the liquid's density, a sharp rise in the supersaturation within the liquid mixture, and the consequent formation of small and uniform particles. GAS is useful for processing of solids which are difficult to solubilize in supercritical fluids, or are sensitive to mechanical handling, such as peptides and proteins.

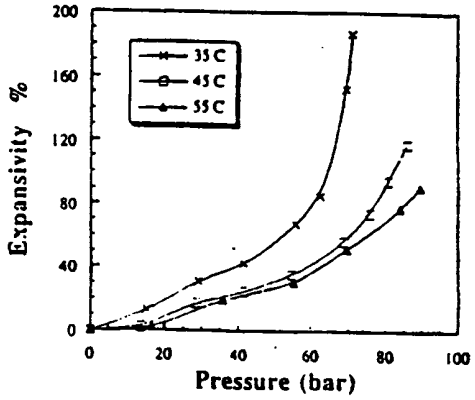

Fig. 4. Expansivity of 90% ethanol/10% DI water with CO_2 as a function of pressure and temperature. The expansivity is defined as the difference between the post- and pre-pressurization liquid phase volumes (the latter at a particular pressure), divided by the initial volume (at the same temperature and atmospheric pressure). (Reprinted from [6], J.W. Tom, G.-B. Lim, P.G. Debenedetti, R.K. Prud'homme, Supercritical Fluid Engineering and Science (Edited by J.F. Brennecke and E. Kiran) ACS Symp. Ser. 514 (1993), 238–257. © 1992 American chemical Society.)

Experimental methods

RESS

Figure 5 shows a typical schematic flow-sheet of a laboratory-scale RESS apparatus [4–6,21]. Typical scales of operation are 20–80 standard l/h of solvent and 0.01 to 1 g/h of solid product, the latter figure being of course a function of the solubility of the solutes in the supercritical solvent. The equipment consists of two main units, extraction (or dissolution) and precipitation. The pure solvent is pumped to the desired pressure and preheated to extraction temperature by circulating through a preheater (consisting either of a coil or a vessel) in a controlled temperature environment. The supercritical fluid is then passed through an extraction unit. This unit is typically a stainless steel column, ~2.54 cm outer

eral advantages over conventional solution formulations. Most systems currently under investigation are injectable microparticulate systems or implantable devices. These formulations consist of peptide or protein particles dispersed within a polymeric matrix. The smaller the particles, the higher the percentage of solids that can be incorporated, and the more uniform the particle distribution within the composite structure. Drug particles in the 1–5 μm size range are ideally required for incorporation into injectable microspheres. Many peptide or protein drugs are highly potent, requiring ng-μg quantities of the compound within the polymeric matrix. Thus, methods for the production of peptide and protein particles on a small scale, with high product yield, high retention of biological activity, and reproducible, easily controllable particle size distribution are required. Conventional techniques such as spray drying, milling, grinding, lyophilization, and controlled precipitation, can in principle, be used to produce small protein particles. Problems associated with these techniques can include shear- or temperature-induced protein inactivation and low yield (spray drying); large (10–50 μm) particles, broad size distributions, and denaturation (milling); electrostatically charged powders and low efficiency towards soft powders (fluid energy grinding); broad distributions (lyophilization); denaturation by organic solvents and the need for a secondary drying step (controlled precipitation with organic solvents). It is therefore important to explore alternative methods that will lead to peptide and protein powders in the < 5 μm size range. The GAS experiments described below suggest that this technique has considerable advantages over alternative technologies for peptide and protein powder formation.

The use of supercritical fluids in biomedical applications is a new, virtually unexplored field. In this article, we explain the fundamentals of the RESS and GAS methods, we review the work done to date in our laboratory, and we suggest future directions of research that we consider to be particularly promising.

Fundamentals

Supercritical fluids

Figure 1 shows a schematic projection of the phase diagram of a pure substance on the pressure-temperature plane. The three lines divide the diagram into three regions: solid, liquid and gas. Along the lines, two phases are in equilibrium and the three states of aggregation coexist at the triple point. The discontinuous transition from liquid to gas ends at the critical point (T_c, P_c). Beyond this point, a low density gas can be compressed into a dense fluid continuously. Strictly speaking, a fluid whose temperature and pressure are simultaneously higher than at the critical point is supercritical. In practice, the term is reserved for the description of fluids in the relative vicinity of the critical point. In this region, the thermophysical properties exhibit very high rates of change with respect to temperature and pressure.

Figure 2 is a typical schematic diagram of the fluid region of a pure substance in the vicinity of its critical point. It shows vapor-liquid coexistence, the critical point (CP), and includes the supercritical region. All quantities are expressed

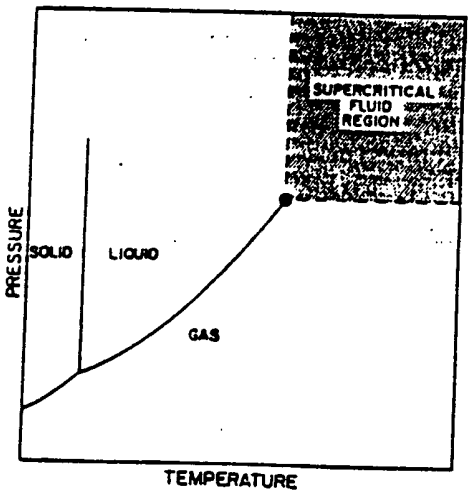

Fig. 1. Pressure-temperature projection of the phase diagram for a pure component (From [35] M. McHugh and V. Krukonis, Supercritical Fluid Extraction. Butterworths, Boston, Massachusetts (1986).).

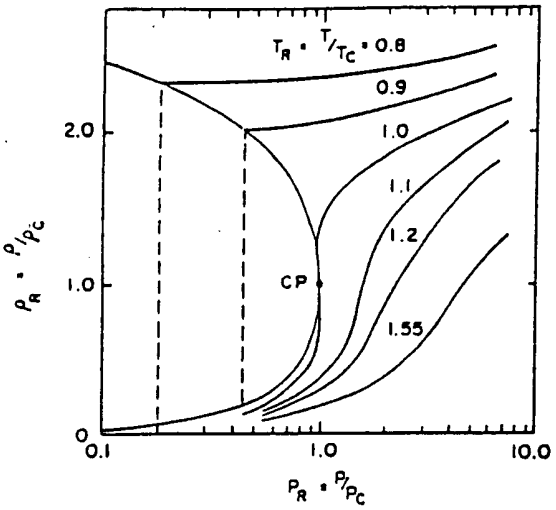

Fig. 2. Schematic phase diagram of the fluid region of a pure substance in reduced density-reduced pressure coordinates. (From [35] M. McHugh and V. Krukonis, Supercritical Fluid Extraction, Butterworths, Boston, Massachusetts (1986).).

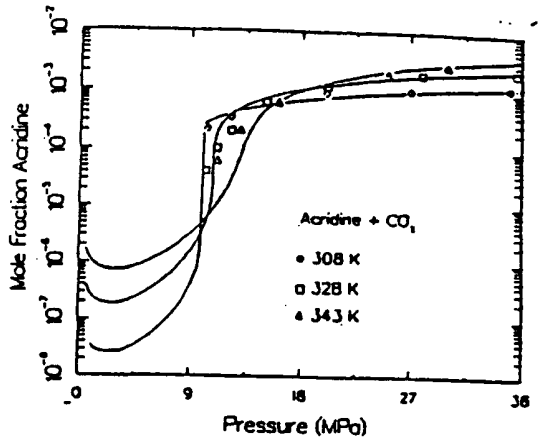

Fig. 3. Solubility of acridine in supercritical carbon dioxide. (From [36] P.G. Debenedetti and S.K. Kumar, AIChE J. 34 (1988) 645-657. Reproduced by permission of the American Institute of Chemcial Engineers © 1988 AIChE).

in reduced units, ie., ratio of a property to its critical point value. The term supercritical is normally reserved for fluids within the approximate temperature and pressure range $1.01 < T/T_c < 1.1$, $1.01 < P/P_c < 1.5$(9). At the critical point, the fluid's compressibility diverges: this can be seen in Fig. 2 from the vertical slope of the critical isotherm at CP, which indicates an infinite rate of change of density with respect to isothermal pressure changes. As a consequence, the entire supercritical region is characterized by very large compressibilities. At the same time, fluid densities can be very close to liquid-like. The distinguishing feature of supercritical fluid is the fact that, though almost liquid-like in density, it possesses a very high compressibility. This allows the use of pressure as a very sensitive means of manipulating and controlling the solvent's characteristics (in particular, its solvent power), spanning the continuum range from gas-like to liquid-like.

The RESS process

Figure 3 shows the solubility of acridine (an organic dye) in supercritical carbon dioxide ($T_c = 304.2$K). It is typical of the phase behavior which characterizes dilute solutions of non-volatile solutes in supercritical solvents. There are three important features to be noticed: (i) a sharp isothermal increase in solubility slightly above the solvent's critical pressure (73.8 bar for CO_2) following the initial solubility decrease, characteristic of ideal gas behavior; (ii) an intermediate regime (known as the retrograde region) where the solubility decreases as the temperature is increased isobarically, indicating exothermic dissolution of a pure solid into the supercritical fluid; (iii) attainment of a solubility plateau at high pressure. The molecular mechanisms which underlie the behavior depicted in Fig. 3 have been the focus of much recent (and ongoing) research [9–18]. The topic is beyond the scope of this review, and the interested reader should consult the above references.

From the standpoint of the RESS process, Fig. 3 shows that non-volatile solutes can be dissolved in compressed supercritical solvents and subsequently recovered by partial expansion (which causes the fluid's density and solvent power to drop sharply). The actual solubility of non-volatile solutes in supercritical fluids can be higher than the value calculated assuming ideal gas behavior at the same temperature and pres-

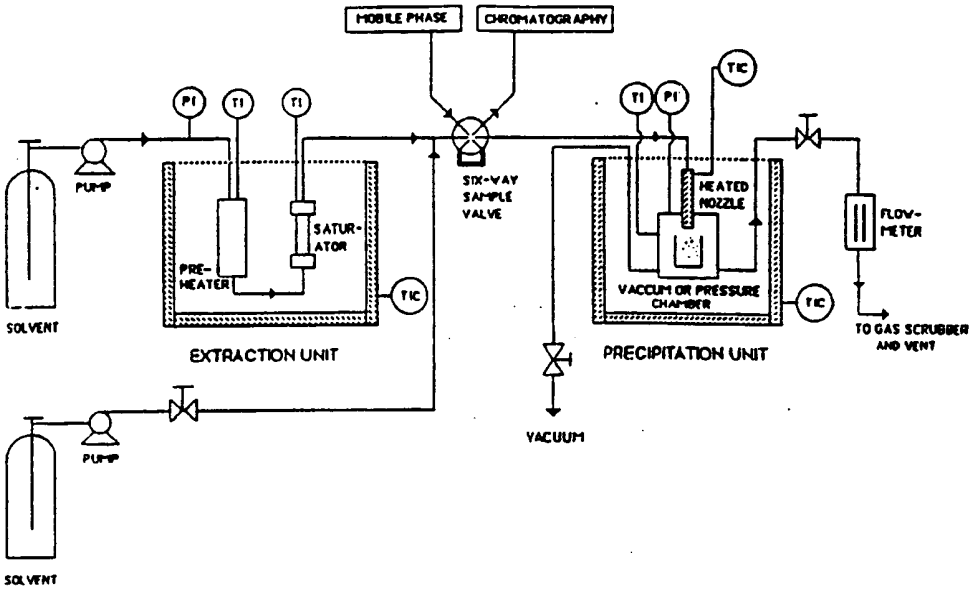

Fig. 5. Experimental apparatus for rapid expansion of supercritical solutions. (From [21], J.W. Tom and P.G. Debenedetti, J. Aerosol Sci. 22 (1991) 555–584.)

dia. × 30 cm length (1" outer dia. × 12" length) [4,25] or a high pressure autoclave, ~300 ml [1] packed with the solute. At such laboratory scales, up to 100 g of solute can be packed with glass wool or beads. For the simultaneous precipitation of multiple solutes, the extraction of solutes from separate extraction units and subsequent mixing of the supercritical solutions prior to expansion allows control over the composition of the powder formed [6,26–27]. Packing the extraction unit with multiple solutes [6] is an alternative to multiple extraction columns. However, the precipitate's composition would be set by the equilibrium solubilities at extraction.

The distinguishing feature of the apparatus shown in Fig. 5 is the possibility of controlling independently the extraction and precipitation pressures and temperatures as well as the solute's concentration prior to precipitation. Pressures are monitored with on-line high-pressure digital gauges (diaphragm or bourdon tube sensors) accurate to within 0.05% and temperatures are measured with thermocouples connected to digital readouts accurate to 0.1°C. Temperature control is an important aspect of the experimental design. Since precipitation can occur with slight changes in temperature, it is important to maintain the lines connecting the extraction and precipitation units at the same temperature as the extraction column. Use of low-critical-temperature-solvents such as carbon dioxide (31.1°C), ethane (32.2°C) or ethylene (9.3°C) permits the use of constant temperature liquid baths (water, silicone oil) in which the extraction and precipitation units are immersed. Connecting lines are either immersed in the bath or wrapped with temperature-controlled heating tape. It is als possible to wrap the extraction unit with temperature-controlled heating tape.

Solute concentration can be varied by diluting the saturated solution exiting the extraction column with pure solvent delivered by another pump. The use of a multi-port high performance liquid chromatography (HPLC) injection valve in the line leading to the precipitation unit allows sampling of the solution for solute concentration. The sample can be analysed on-line prior to precipitation by directing it to an appropriate chromatography system or collected in a sample vial for later analysis. Available chromatography

systems include high performance liquid chromatography using an ultraviolet detector for small organic molecules, gel permeation chromatography using a refractive index detector for proteins and polymers, and gas chromatography using a flame-ionizing detector for volatile organic compounds.

In the precipitation unit, the supercritical solution is expanded across a nozzle or a calibrated orifice. Some of the expansion configurations tested have been 2–30 mm length, 25–60 μm inner diameter tubing [26–28] and 40 mm length, 200 μm inner diameter tubing [29]. Laser drilled pinpoint orifices of 15–30 μm diameter [4–6,25] and larger orifices of 1600 μm [25] have also been investigated. The expansion device's temperature is controlled with a variable resistance cable heater which is regulated by an indicator controller. The heating of the nozzle up to an adequate pre-expansion temperature is necessary to prevent phase changes in the solvent (i.e., condensation, freezing) upon expansion. Particle collection by impaction onto a plate [26–27], into a glass beaker [4] and dispersion into an aqueous colloidal gel [25] have been employed. Dispersing the precipitate into a suspending medium reduces the amount of agglomeration.

A stainless steel chamber designed for high pressures can be used to study precipitation following partial expansion to intermediate pressures [4]. Such a unit can be designed with glass or sapphire windows both to observe powder collection and to make unobtrusive measurements of particle sizes using optical techniques. After depressurization, the solvent is released as a dilute gas. Instantaneous flow rates can be determined with gas flow meters and total flow can be found with a flow totalizer (wet or dry test flow meter). Pressure control is done with a micrometering valve located at the crystallizer's exit in the precipitation unit.

To date, most particle characterization has been performed via off-line methods. Optical and scanning electron microscopy [2,4–6,26]; particle sizers which measure resistance changes proportional to particle volume (i.e., the Coulter Counter and the Elzone particle analyser: [4,25]; and nitrogen gas adsorption, which measures surface area (i.e., BET: [25,30]) have been used to analyse morphology and size distribution. Changes in the crystallinity or the amorphous nature of the precipitates have been examined using X-ray diffraction for non-polymeric organic molecules [2,4,6,26], and differential scanning calorimetry (DSC) for polymers [5,29]. Infrared spectroscopy and NMR were utilized to verify the chemical composition of the material [5–6,25]. Fluorescence spectroscopy has been used to determine the homogeneity of precipitates from multiple solutes [26].

GAS

A schematic diagram of the continuous GAS apparatus used recently for protein powder formation with CO_2 as supercritical anti-solvent [6,8] is shown in Fig. 6. The apparatus consists of four sections: see-through crystallizer (ca. 75 ml); protein solution feeding unit; anti-solvent supply system; and depressurizing section. During GAS operation, the anti-solvent is pumped to the top of the crystallizer by a high pressure

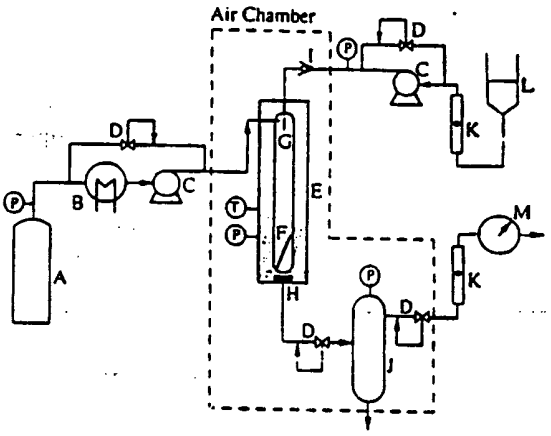

A. Carbon Dioxide
B. Cooler
C. High Pressure Pump
D. Back Pressure Regulator
E. Crystallizer
F. Glass Sampler
G. Nozzle
H. Metal Filter
I. Check Valve
J. Depressurizing Tank
K. Rotameter
L. Protein Solution
M. Dry Test Meter

Fig. 6. Experimental apparatus for gas anti-solvent precipitation.

pump whose discharge pressure is controlled by a back pressure regulator. Before entering the pump, the anti-solvent is cooled down to ca. 0°C using a circulation cooler to prevent cavitation. In the experiments of Yeo et al. [8], pressure in the crystallizer was maintained at 86.2 bar by means of a back pressure regulator. The crystallizer, depressurizing tank, and associated tubing are installed in an insulated air chamber whose temperature is controlled by a temperature controller, strip heaters, and circulating fans. Once the system reaches steady state, the protein solution is pumped to the crystallizer through a nozzle. To produce small liquid droplets in the nozzle, the liquid solution is pumped at a pressure ca. 20 bar higher than the crystallizer's operating pressure. The nozzle (ca. 30 μm diameter, 0.24 mm thickness, platinum) is installed at the top of the crystallizer, so that both the protein solution and supercritical anti-solvent flow continuously and in downward cocurrent mode through the crystallizer. Sub-millimeter liquid droplets are sprayed into a continuum of supercritical anti-solvent. Protein particles produced from the expansion and evaporation of the liquid droplets are collected on a glass slide and on a metal filter (0.5–2.0 μm) located at the bottom of the crystallizer. The fluid mixture (largely supercritical anti-solvent plus residual protein-depleted solvent) leaves the crystallizer and flows to a 150 ml depressurizing tank. After collection of a sufficient among of protein, liquid solution flow ceases and pure anti-solvent continues to flow through the crystallizer to remove residual solvent on the particles. Typical flow rates are 8.0 standard liters per min for the supercritical anti-solvent and 0.3 ml/min for the protein solution. In a typical experiment with a 5 mg/ml solution of insulin in dimethyl sulfoxide [8], the precipitation stage lasted 0.7 h, and 25 mg of insulin were collected on both the glass slide and the metal filter.

Previous work

RESS processing of bioerodible polymers

Tom and Debenedetti [5] studied the RESS-processing of poly(hydroxy acids) [poly(L-lactic acid) (L-PLA); poly(D,L-lactic acid) (DL-PLA); poly(glycolic acid) (PGA)] with CO_2 and CO_2-rich mixtures. Commercial L-PLA (Boehringer Ingelheim; L-104; lot nos. EC8802 and 93015) was used in the solubility and nucleation experiments. Commercial DL-PLA (Boehringer Ingelheim; R-104; lot no. 93016) and PGA (Boehringer Ingelheim; G-110; lot no. 95028) were also processed by RESS. The structure, molecular weight, and polydispersity of the commercial polymers are shown in Table 1.

The dissolution of L-PLA in supercritical CO_2 is a necessary condition for its processing by RESS. Since commercial L-PLA, which is polydisperse, is commonly used in the production of polymeric microspheres for drug release, the total solubility of the polydisperse material was investigated. Polydispersity has a significant impact on the progress of the experiments. Lower molecular weight polymers are preferentially extracted from a polydisperse sample. Thus, the molecular weight distributions of the polymer in the column and the precipitate change over time.

During collection of samples, the CO_2 in the sample loop was evaporated. Chloroform was used to flush the polymer from the same loop, and CO_2 was then used to displace any remaining chloroform in the sampling lines. The sample was concentrated for analysis by gel permeation chromatography (GPC). The samples were passed through a polystyrene/divinylbenzene column with chloroform as the mobile phase, monitored with a refractive index detector, and the peaks were recorded and integrated automatically. The concentration of the sample was correlated with the area of the peaks. In solubility experiments where the amount of CO_2 passed per g of L-PLA initially in the column was high (> 100 total standard liters per gram, TSLPG), the reported solubilities are averages of three to six samples taken 40–60 min apart. Under these conditions, the total solubility was found to be virtually independent of time. The flow rate of carbon dioxide exiting the apparatus during the solubility experiments was typically 0.5 standard liters per min (SLPM). No change in solubility was observed for flow rates up to 1 SLPM.

TABLE I

Characteristics of the polymers used in RESS-processing study [5]

Polymer	Structure	T_m (°C)	M_w	M_w/M_n
L-PLA	$H[-OC^*H(CH_3)C(O)-]_nOH$	137	5500	2.0
DL-PLA	$H[-OCH(CH_3)C(O)-]_nOH$	na	5300	1.9
PGA	$H[-OCH_2C(O)-]_nOH$	203	6000[b]	2.0[b]

[a]Asterisk denotes asymmetric carbon.
[b]Data from [31].

The total solubility is a function of the cumulative amount of solvent used normalized by the amount of polymer initially present in the column. With different quantities of polymer packed in the column, the solubility was measured over time. It was found that if the processing time was converted to cumulative amount of CO_2 used per unit mass of polymer initially loaded in the column, master curves resulted that show how the total solubility and the molecular weight of the extracted L-PLA evolve in time at given operating conditions (Fig. 7). The master curves in Fig. 7 are for extraction conditions of 55°C and 250 bar. The molecular weight in Fig. 7b is that of the highest molecular weight peak from the GPC curve. The inserts refer to the amount of polymer loaded initially in the column. The solubility in Fig. 7a is the solubility of all the oligomers extracted. While there is considerable scatter in the data, the following trends are obvious: (1) the solubility drops sharply as TSLPG increases from 0 to ~20; (2) the solubility flattens to <0.03 wt% above 20 TSLPG; and (3) the molecular weight of the extracted L-PLA increases with processing time. The drop in solubility reflects the extraction of fractions with progressively higher molecular weight.

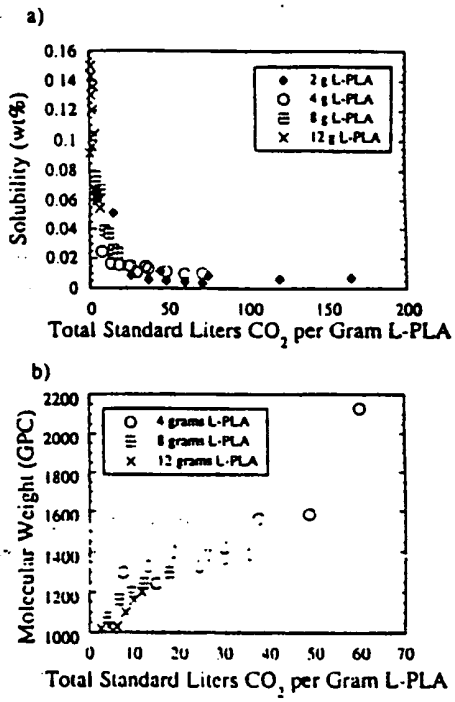

Fig. 7. Master solubility curve (a) and master molecular weight curve (b) for L-PLA at CO_2 extraction conditions of 55°C and 250 bar. (Reprinted from [5], J.W. Tom and P.G. Debenedetti, Biotechnol. Prog. 7 (1991) 403-411. © 1991 American Chemical Society.)

The solubility of commercial L-PLA (TSLPG>40) in pure carbon dioxide, and in carbon dioxide containing 1 wt% acetone was measured at temperatures of 45, 55 and 65°C and pressures of 150, 200, 250 and 300 bar. The data are shown in Fig. 8. Acetone was selected as a cosolvent because at 50–60°C it dissolves up to 25–30 wt% L-PLA [31]. Solubilities in pure CO_2 ranged from 0.01 to 0.07 wt%. Significant increases were observed with the addition of 1 wt% acetone. Solubilities ranged from 0.05 to 0.37 wt%. The co-solvent-induced solubility enhancement at a given process condition was typically ~500%.

After 260 TSLPG were passed through the column (i.e., after completing the above solubility

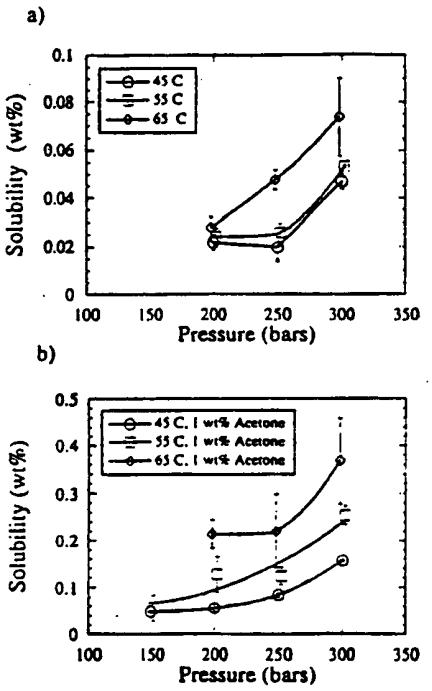

Fig. 8. Solubility of L-PLA in CO_2 at temperatures of 45, 55 and 65°C and pressures of 200, 250 and 300 bar (a) and in CO_2 with 1 wt% acetone at temperatures of 45, 55 and 65°C and pressures of 150, 200, 250 and 300 bar (b). (Reprinted from [5], J.W. Tom and P.G. Debenedetti, Biotechnol. Prog. 7 (1991) 403-411. © 1991 American Chemical Society.)

studies), the molecular weight (M_w) of the polymer in the column had increased from 5500 to ~6200. The change in the polydispersity (M_w/M_n) was undetectable. The GPC traces of L-PLA extracted at small and large values of TSLPG (i.e., at short and long times) provide information on the distribution of the precipitated polymer's molecular weight. The commercial polymer had a broad peak eluting at a time corresponding to ~5000 molecular weight. At short times (TSLPG < 20), the main peak of the extracted polymer eluted at 1100 molecular weight and a smaller peak eluted at 600–700 molecular weight. At long times (TSLPG > 100), the high-molecular-weight peak was shifted to >2000 and a larger peak accounting for 60–70% of the total solubility eluted at molecular weight of <1000. Thus, as TSLPG increases, the higher molecular weight peak increases in molecular weight, but contributes less to the total solubility. The total solubility was taken as the sum of these first two peaks. A third peak was usually observed at a molecular weight of ~150; it corresponds to the dimer of lactic acid (dilactide, $M_w = 144$. The dilactide forms readily from the monomer. The quantitiy of dilactide detected throughout the experiments was accounted for from the monomer content of the commercial polymer (3%). The concentration of dilactide decreased to 3% at high TSLPG (>300).

Precipitation of the commercial L-PLA by using CO_2 with 1 wt% acetone produced a variety of L-PLA morphologies, as shown in Fig. 9. Both sets of polymer particles in Fig. 9 were produced at high TSLPG (>190) by extraction at 55°C and 200–230 bar. The pre-expansion temperatures were 75–100°C. The supercritical solution was expanded to 10–5 bar; bulk crystallizer temperatures of 15–37°C in case 1, and 49–52°C in case 2, were used. In case 1, microparticles of 10–25 μm were obtained; in case 2, dendrites of up to several hundred μm were formed. However, the elementary particles forming the dendrites were similar in shape to the particles obtained in case 1. A possible explanation for dendrite formation is the difference in the bulk crystallizer temperature; at the higher temperature, the polymer particles are softened and may fuse upon contact, while at the lower temperature the polymer is glassy and particles do not adhere easily. The duration of these experiments was also different: 1.25 h in case 1, and 2.5 h in case 2.

The effect of preexpansion temperature on L-PLA precipitation from CO_2 and CO_2-acetone solutions was studied at high TSLPG. At preexpansion temperatures of 60–100°C, the particles resembled deflated balloons (Fig. 9). However, at a preexpansion temperature of 120°C, both microspheres and spheroidal particles (<10 μm) were formed. A typical microsphere is shown in Fig. 10. All microspheres were less than 10 μm. The mechanisms that contribute to the formation of microspheres vs. microparticles are currently under investigation.

The hydrolysis rate of precipitated L-PLA was

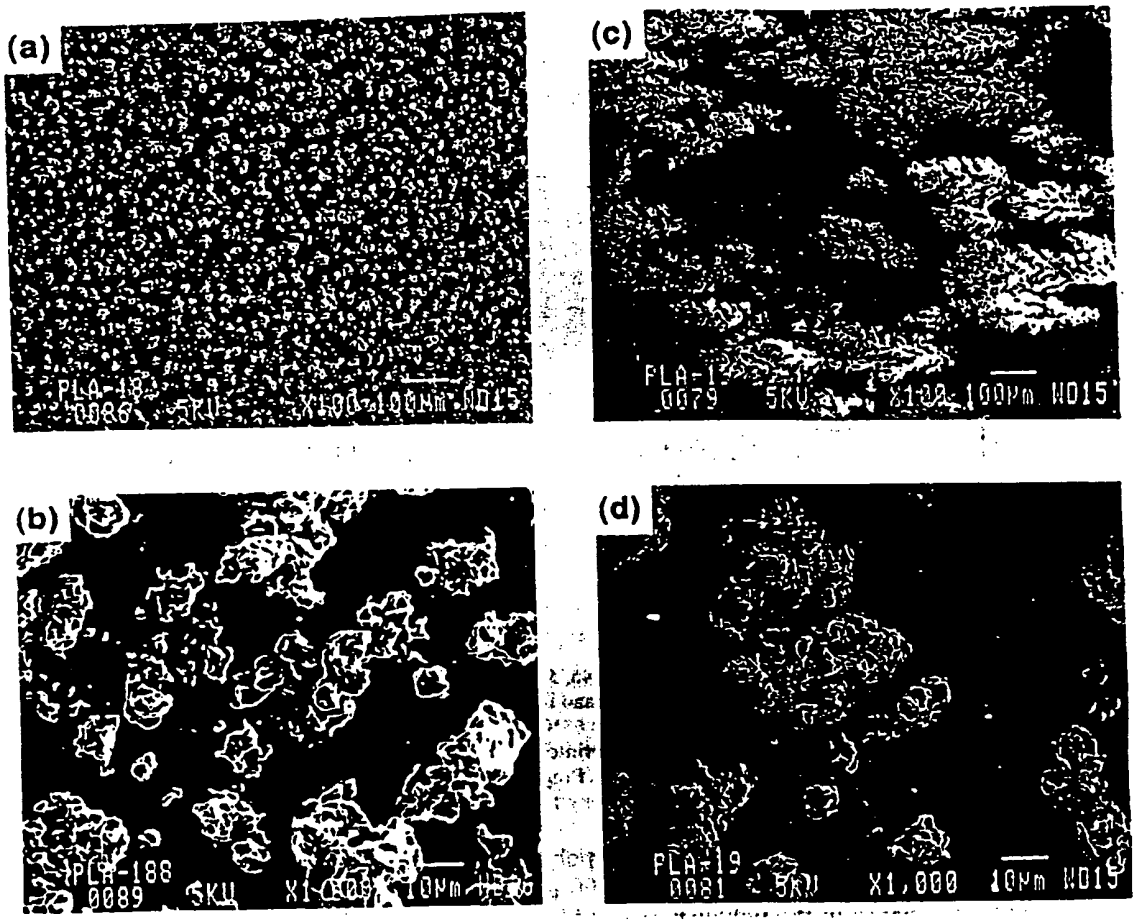

Fig. 9. SEM of L-PLA particles from RESS using CO_2 with 1 wt% acetone at extraction conditions of 55°C and 200–250 bar. Crystallizer temperature 15–37°C (a,b), crystallizer temperature 49–52°C (c,d). (Reprinted from [5], J.W. Tom and P.G. Debenedetti, Biotechnol. Prog. 7 (1991) 403–411. © 1991 American Chemcial Society.)

compared with that of the commercial polymer. The polymer (10–40 mg) was suspended in 100–125 ml of aqueous phosphate buffer solution (pH 7.4). The buffer was placed in a 37°C shake bath for up to 400 h. The concentration of L-lactic acid was monitored by reacting an aliquot of the buffer solution with nicotinamide adenine dinucleotide (NAD) and lactate dehydrogenase. The aliquot's ultraviolet absorbance at 340 nm correlated linearly with the L-lactic acid concentration from a standard calibration curve. The weight percent degraded (defined as 100-times the ratio of the L-lactic acid's weight present in the solution at any given time to the initial weight of the polymer originally placed in the solution) was measured over time for commercial and precipitated polymer (Fig. 11). Commercial L-PLA degraded at a slow and constant rate; after 300 h, only 10 wt% of material was lost. L-PLA precipitated at TSLPG < 20 showed a fast rate of hydrolysis in the first 50 h after which it exhibited a rate of degradation similar to that of commercial L-PLA. This initial fast rate of hydrolysis is due to the higher concentration of low molecular

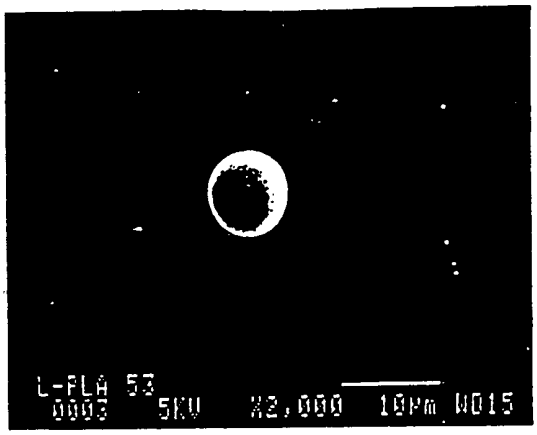

Fig. 10. SEM of L-PLA microsphere from RESS using CO_2 with 1 wt% acetone at extraction conditions of 55°C and 240–250 bar and a preexpansion temperature of 120°C (Reprinted from [5]. J.W. Tom and P.G. Debenedetti, Biotechnol. Prog. 7 (1991) 403-411. © 1991 American Chemical Society.)

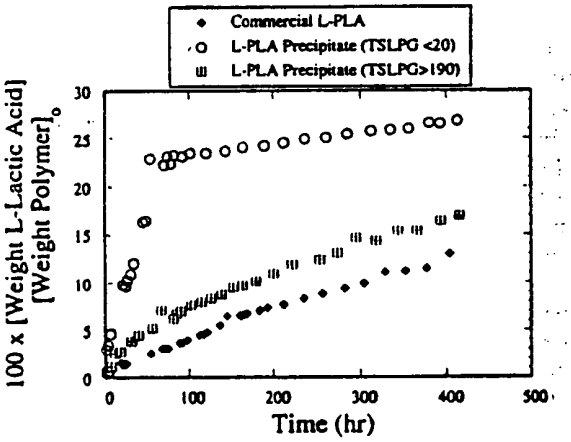

Fig. 11. Hydrolysis rate for commercial and precipitated L-PLA. The y-axis gives 100-times the weight of L-Lactic acid in solution divided by the weight of L-PLA initially in solution. (Reprinted from [5], J.W. Tom and P.G. Debenedetti, Biotechnol. Prog. 7. (1991) 403-411. © 1991 American Chemical Society.)

weight material and dilactide in the precipitate formed at low TSLPG. L-PLA precipitated at TSLPG > 190 showed a rate of hydrolysis similar to that of the commercial L-PLA. After 300 h, only 14 wt% of the polymer degraded.

In summary, three general types of precipitate were produced from commercial L-PLA. The initial precipitate was solid and crystalline. It consisted of low molecular weight polymer and dilactide. The length of some of the needles indicates that there was growth of material on the glass substrate. After the initial solid (and mostly crystalline) material, a viscous and clear precipitate was produced. This low molecular weight material has a T_g below room temperature and is mostly amorphous. After the viscous material, microparticles and microspheres with higher T_m were obtained.

Commercial DL-PLA was received as solid aggregates several inches in size and was ground by mortar and pestle to irregular-sized particles (100–300 μm) before charging to the extraction column. DL-PLA is soluble in many common organic solvents [acetone, acetonitrile, chloroform, ethyl acetate and others [31]]. It has been studied for release periods of up to 30 days [32]. DL-PLA was found to be soluble in supercritical CO_2. Rapid expansion of supercritical CO_2 solutions containing DL-PLA produced irregularly shaped particles that were fairly uniform in size (10–20 μm). The extraction and precipitation conditions were 55°C and 200 bar, and 15–25°C and 0.5 bar, respectively. The preexpansion temperature was 82–85°C. The particles were collected at <7 TSLPG.

The amount of material collected during precipitation indicated that the solubility (weight percent) was of the same order of magnitude as that of L-PLA. There was evidence of significant CO_2 sorption by DL-PLA since there was movement of polymer within the column. The changes in morphology of precipitated DL-PLA with processing time have yet to be explored. GPC analysis showed that the material contained ~60–70% polymer (M_w ~ 900) and 30–40% dilactide. The infrared spectrum confirmed that the material was DL-PLA, while the NMR spectrum indicated the presence of both DL-PLA and dilactide.

PGA is insoluble in most organic solvents. It has been reported to be soluble in but a few solvents, such as hexafluoro-2-propanol, hexafluoroacetone sesquihydrate, and phenoltrichloro-

phenol [32]. Because of PGA's poor solubility and the consequent difficulty in finding a common solvent for PGA and the drug of interest, there are very few methods for the fabrication of PGA into dosage forms for controlled drug delivery applications [32]. Approaches that have been tried to date for the processing of PGA include melt pressing the polymer with the drug at temperatures above 200°C [32] and mechanical compression of PGA with the drug [33]. Most recent work involving PGA has focused on copolymers of PGA with either DL-PLA or L-PLA. The copolymers are completely amorphous and soluble in a range of organic solvents. However, PGA by itself is useful for drug delivery applications over periods of up to 10 days [32]. Studies of longer delivery periods have not been done, but the concept should be feasible since the half life of PGA can be similar to that of L-PLA, depending on the curing rate of PGA [32]. PGA was found to be soluble in supercritical CO_2 at 55°C and 180–200 bar. The PGA precipitate from RESS consisted of regular-shaped particles (ovals and rectangles), 10–20 μm in length, and some needles of up to 40 μm length. Polarized microscopy showed that the precipitate was highly crystalline. The pre-expansion temperature was 80–82°C, the precipitation conditions were 15–22°C and 7–9 bar and the particles were collected at < 50 TSLPG.

The solubilization and precipitation of three biocompatible homopolymers (L-PLA, DL-PLA, and PGA) with supercritical CO_2 suggests that the complete range of PGA/PLA-based polymers can be processed by RESS. The molecular weight of the precipitated polymers is lower than that of the commercial polymer. Thus, RESS with CO_2 may be limited to low molecular weight poly(hydroxy acids). However, other supercritical solvents such as chlorofluorohydrocarbons can easily dissolve a range of polymers of high molecular weight [29].

RESS coprecipitation of a drug and a polymer

The first example of polymer-drug microsphere produced in a process involving supercritical solvents was patented by Mueller and Fischer [34]. In their process, supercritical CO_2 was contacted with a methylene chloride solution of drug (clonidine hydrochloride) and DL-PLA. Our work differs from that of Mueller and Fischer [34] in that we dissolve the polymer and drug in a supercritical fluid directly, avoiding the use of organic solvents. The coprecipitation experiments described here [6] illustrate the variati n in the precipitate's morphology and composition that can result from slight changes in the relative amounts of drug and polymer initially loaded into the extraction unit. Experiments were done both with a single column packed with both solutes, or with two columns operating in parallel [6]. Extraction conditions of 200–250 bar and 55°C were used. 13.5 g of polymer (DL-PLA) and 0.5 g of drug (lovastatin; an anti-cholesterol drug, $M_w = 404$) were intimately mixed in column 1 while column 2 was packed with 15 g of lovastatin. After passing ~200 TSLPG of supercritical CO_2 at 200–250 bar and 55°C through column 1 to extract the low-molecular-weight oligomers and dilactides, solid particles were produced. As in the case of L-PLA, the polydispersity of the polymer leads to preferential extraction of low-molecular-weight material early in the processing. The low-molecular-weight polymer forms either needles or a viscous, low-T_g precipitate [5].

One coprecipitation experiment was then performed by flowing CO_2 at 200 bar and 55°C through column 1, with column 2 inactive. With preexpansion temperatures of 75–80°C, a range of particles was obtained. Microspheres containing single lovastatin needles (Fig. 12), as well as egg-shaped polymer particles enveloping lovastatin needles (Fig. 13), microspheres without protruding needles, and needles without a polymeric enclosure were produced. Proton NMR of the precipitate showed the presence of lovastatin and DL-PLA exclusively, with the lovastatin concentration estimated at 20 wt%.

In a second experiment, both columns were used. Extraction conditions of 190–220 bar and 55°C for column 1, and 35°C for column 2 were used, with preexpansion temperatures of 75–85°C. Large microparticles containing multiple needles of lovastatin were obtained. Proton NMR

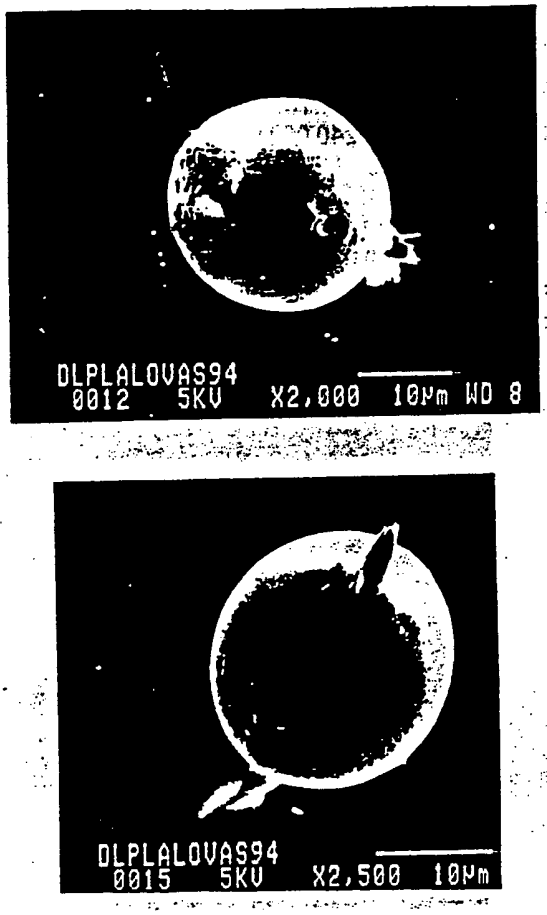

Fig. 12. SEM of DL-PLA microspheres with embedded lovastatin needles from RESS using CO_2 at extraction conditions of 55°C and 200 bar and a preexpansion temperature of 80°C. (Reprinted from [6], J.W. Tom, G.-B. Lim, P.G. Debenedetti, R.K. Prud'homme, in: Supercritical Fluid Engineering and Science (Edited by J.F. Brennecke and E. Kiran) ACS Symp. Ser. 514 (1993), 238–257. © 1992 American Chemcial Society.)

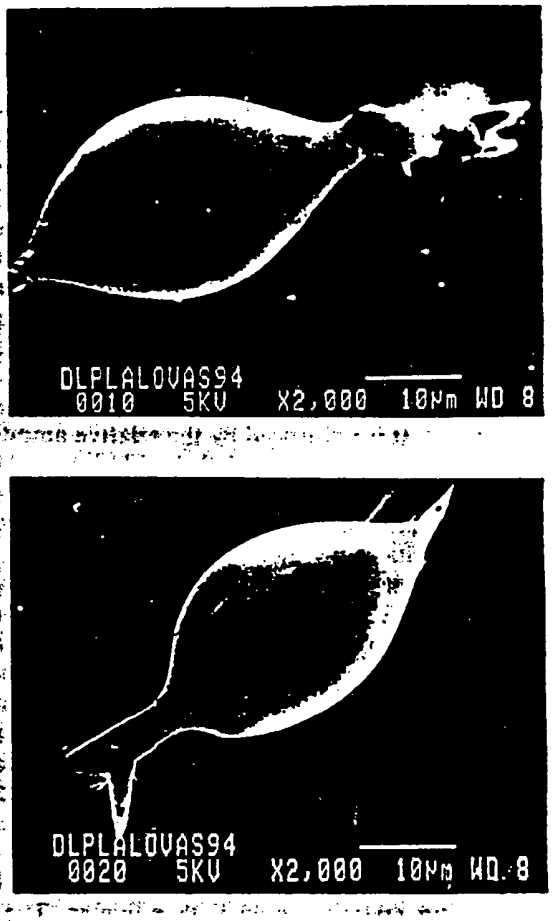

Fig. 13. SEM of DL-PLA microparticles with embedded lovastatin needles from RESS using CO_2 at extracti n conditions of 55°C and 200 bar and a preexpansion temperature of 80°C. (Reprinted from [6], J.W. Tom, G.-B. Lim, P.G. Debenedetti, R.K. Prud'homme, Supercritical Fluid Engineering and Science (Edited by J.F. Brennecke and E. Kiran) ACS Symp. Ser. 514 (1993), 238–257. © 1992 American Chemical Society.)

of this precipitate revealed the presence of ca. 27 wt% lovastatin.

In a third experiment, column 1 was packed with 3.6 g of a reprecipitated DL-PLA/lovastatin mixture. The material remaining in column 1 after the first two experiments was reprecipitated using acetone and water to produce polymer of higher molecular weight and lower polydispersity. GPC showed the polymer to have a M_w of ca. 10 000. RESS coprecipitation of material in column 1 at CO_2 extraction conditions of 200 bar and 55°C and pre-expansion temperature of 80°C resulted in a solid network consisting of intertwining fibers of 2–5 µm width (lovastatin needles joined by a continuous polymer network). Proton NMR of the solids showed approximately 36 wt% lovastatin, the preferential extraction of lovastatin over DL-PLA being

due to the polymer's increased molecular weight. The network morphology is similar to that obtained by RESS of polystyrene in supercritical pentane [1].

While a quantitative understanding of events leading to the type of particles shown in Figs. 12 and 13 remains a distant goal, it seems reasonable to assume that nucleation and growth of drug crystals occurred first, and that these particles subsequently acted as nucleating sites for the polymer. Thus, the joint evolution of the respective supersaturations of drug and polymer along the expansion path appears to be very important. It is influenced by the relative amounts of drug and polymer initially in solution, and hence by such variables as initial column loadings, polymer molecular weight, and extraction conditions.

These exploratory experiments show the feasibility of using RESS to coprecipitate a polymer and a drug. The results are part of ongoing investigations in our laboratory aimed at developing optimal process conditions for RESS coprecipitation of polymer-drug microspheres with consistent composition and desirable drug distribution. Various morphologies have been obtained under different polymer and drug loadings in the columns. The most important result to date is the formation of microparticles consisting of lovastatin crystals coated with polymer. The ideal polymer-drug particles for controlled drug delivery would be microspheres containing many small, uniformly dispersed drug particles, rather than single needles. This requires that the polymer precipitate before the drug particles are allowed to grow into large crystals. Work is in progress to find optimum process conditions that will lead to this desired morphology. Experimental variables under study include extraction conditions, as well as use of capillary tubes of varying length as expansion devices. Segregation of solutes into two columns should afford better control over the coprecipitation.

Formation of protein powders by GAS precipitation

The GAS process has been used to form insulin powders from DMSO and dimethyl formamide (DMFA) [8], and catalase and insulin powders fr m ethanol-water mixtures [6]. In the experiments of Tom et al. [6], catalase (bovine liver; $M_w \sim 240\,000$) or insulin (Zn, low endotoxin; $M_w \sim 6000$) were dissolved in a 90% ethanol/10% DI water mixture (typical protein concentration was 0.1 mg/ml). The solution was adjusted to a pH of 3.0–3.5 with 1 N HCl. Filtra-

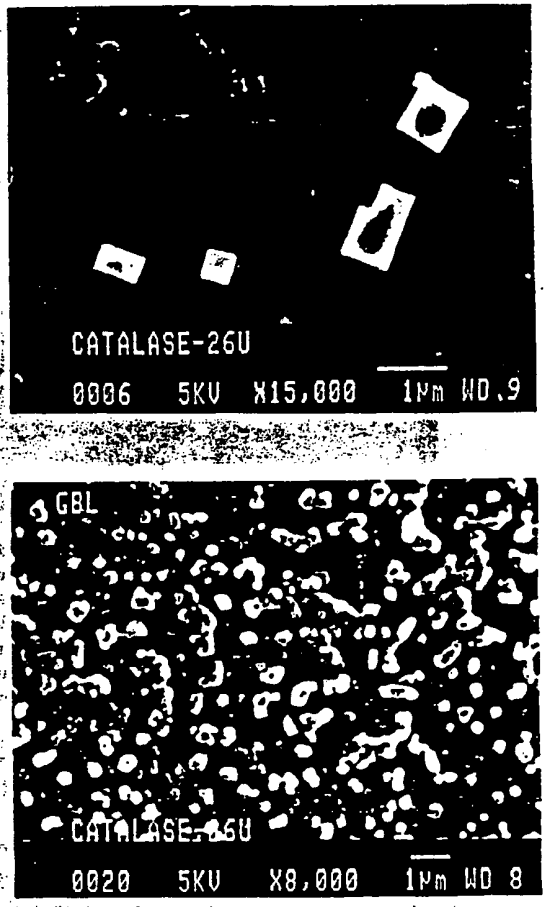

Fig. 14. SEM of catalase particles formed by GAS precipitation. (Reprinted from [6]. J.W. Tom. G.-B. Lim. P.G. Debenedetti. R.K. Prud'homme. in: Supercritical Fluid Engineering and Science (Edited by J.F. Brennecke and E. Kiran) ACS Symp. Ser. 514 (1993). 238–257. © 1992 American Chemical Society.)

tion (0.2 μm nylon filters) removed undissolved pr tein particles. The GAS experiments were done at 35°C, a condition that combines high expansivity (see Fig. 4) with the low temperatures that are desirable for protein processing. In these experiments, the protein solution and supercritical CO_2 were pumped cocurrently into the crystallizer, which was held at 90 bar. At 35°C and above 80 bar, significant evaporation of ethanol into the supercritical phase occurs. Expansivity is only a property of the liquid phase as long as no vaporization into the gas phase occurs. When evaporation takes place, it is more appropriate to talk about the equilibrium mole fractions of solvent in the gas, and of the gas in the solvent. These quantities were not measured. However, operation under conditions where substantial evaporation occurred was chosen so as to facilitate as complete as possible a removal of the liquid phase from the process.

In the catalase experiment, the protein solution (0.1 mg/ml) and CO_2 flow rates were 0.35 ml/min and 16.9 SLPM, respectively. The protein solution was introduced through a 20 μm nozzle. Catalase particles collected on the glass slide were either spherical or rectangular, and approximately one micron in size (Fig. 14). In the insulin experiment, the protein solution (0.1 mg/ml) was introduced through the same nozzle at 0.39 ml/min and CO_2 was charged at a rate of 18.2 SLPM. The insulin particles were collected on a filter at the bottom of the crystallizer. Two types of insulin particles were obtained: microspheres (≤ 1 μm) and thick needles of ~ 5 μm length and 1 μm in width. The two types of particles were found in separate areas of the fil-

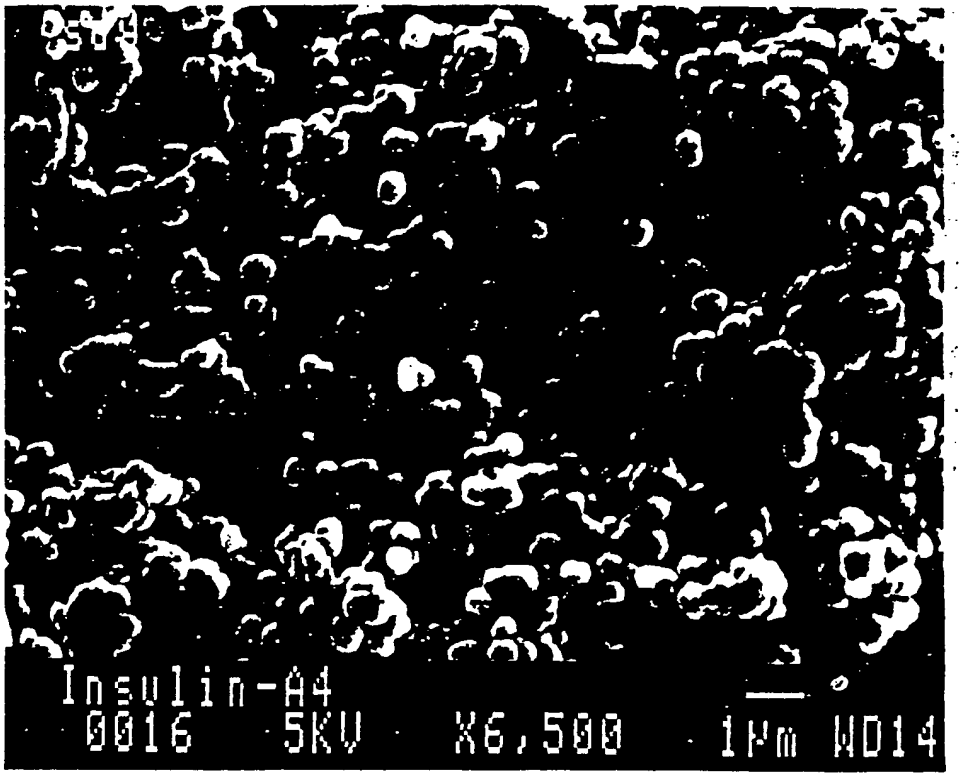

Fig. 15. SEM of insulin particles formed by GAS precipitation.

ter, although some microspheres were found interspersed with the needles.

In the more recent experiments of Yeo et al. [8], bovine insulin was dissolved in DMSO and DMFA. The range of conditions tested included changes in temperature (25, 35°C) protein concentration (5, 15 mg/ml); solvent (DMSO, DMFA), and mode of operation (continuous, semi-batch). In continuous co-current operation (similar to that used by Tom et al. [6]), the flow rates were 8 SLPM (CO_2) and 0.3 ml/min (insulin solution), and powders with mean particle size in the 2–3 μm range were obtained in every case, regardless of process conditions. Figure 15 shows insulin particles produced by GAS precipitation at 35°C and 86 bar from a DMSO solution (5 mg/ml). Some aggregation and fusing of individual particles is observed by SEM. Coulter counter particle size distribution analysis performed after mild sonication (4 min in methylene chloride) confirmed that these were loose aggregates and that the mean particle size was 2–3 μm. At least 90% of the particles were smaller than 4 μm, and 10% of the particles were smaller than 1 μm in all continuous experiments. Considerably larger particles resulted when a stagnant insulin solution was slowly pressurized with CO_2 (0.57 bar/min), suggesting the interesting possibility of controlling the particle size through the rate of solvent addition.

The biological activity of GAS-processed insulin powders was determined by animal tests [8]. The processed insulin's activity (i.e., the degree to which it lowered blood glucose level: typically from 120 to 30 mg/dl in 2 h) was found to be indistinguishable from that of the original material.

Conclusions

RESS can in principle be used to produce solvent-free drug-loaded microspheres. Coating of drug needles with a bioerodible polymer has been achieved, but considerable work remains to be done before finely dispersed drug powders can be reliably and reproducibly incorporated in the polymer matrix using a rapid expansion. The current level of understanding of the complex process that take place during RESS coprecipitation (homogeneous nucleation, heterogeneous nucleation, particle growth and coagulation) is quite primitive. A better grasp of the underlying physics is needed as a guide to a more rational design of the process.

GAS is a very promising route to ultrafine and biologically active protein powders. Addition of a bioerodible polymer to the protein solution could result in peptide-loaded microspheres. This possibility is currently under investigation. At present GAS is restricted to solvents with minimum-to-nil water content.

The biomedical applications of supercritical fluids remain virtually unexplored. The use of substances such a carbon dioxide allows processing of labile materials at mild temperatures, and eliminates the need for liquid solvents. We have presented selected examples of ongoing RESS and GAS work in our laboratory. Additional techniques are likely to emerge as interest in this promising new field grows.

Acknowledgements

PGD gratefully acknowledges the support of Enzytech, Inc.; the National Science Foundation (Grant CTS-9000614); the Camille and Henry Dreyfus Foundation (1989 Teacher-Scholar Award); the John Simon Guggenheim Memorial Foundation (1991 Fellowship); and thanks Professor John M. Prausnitz for his hospitality during a sabbatical leave at the Department of Chemical Engineering at the University of California at Berkeley. JWT is a National Science Foundation Pre-Doctoral Fellow. The lovastatin was generously donated by Merck Research Laboratories (Rahway, NJ).

References

1. D.W. Matson, J.L. Fulton, R.C. Petersen and R.D. Smith, Rapid expansion of supercritical fluid solutions: solute formation of powders, thin films, and fibers, Ind. Eng. Chem. Res. 26 (1987) 2298–2306.
2. K.A. Larson and M.L. King, Evaluation of supercritical fluid extraction in the pharmaceutical industry, Biotechnol. Prog. 2 (1986) 73–82.

3 H. Loth and E. Hemgesberg, Properties and dissolution of drugs micronized by crystallization from supercritical gases, Int. J. Pharm. 32 (1986) 265–267.

4 R.S. Mohamed, D.S. Halverson, P.G. Debenedetti, R.K. Prud'homme, Solids formation after the expansion of supercritical mixtures, in: K.P. Johnston and J.M.L. Penninger (Eds.), Supercritical Fluid Science and Technology, ACS Symp. Ser. 406, American Chemical Society, Washington, DC, 1989, pp. 355–378.

5 J.W. Tom and P.G. Debenedetti, Formation of bioerodible polymeric microspheres and microparticles by rapid expansion of supercritical solutions, Biotechnol. Prog. 7 (1991) 403–411.

6 J.W. Tom, G.-B. Lim, P.G. Debenedetti, R.K. Prud'homme, Applications of supercritical fluids in controlled release of drugs, in: J.F. Brennecke and E. Kiran (Eds.) Supercritical Fluid Engineering Science, ACS Symp. Ser. 514, American Chemical Society: Washington, DC, 1993 pp.238–257.

7 P.M. Gallagher, M.P. Coffey, V.J. Krukonis and N. Klasutis, in: K.P. Johnston and J.M.L. Penninger (Eds.) Supercritical Fluid Science and Technology, ACS Symposium Series 406, American Chemical Society: Washington, DC, 1989, pp. 334–354.

8 S.D. Yeo, G.-B. Lim, P.G. Debenedetti and H. Bernstein, Production of microparticulate protein powders using a supercritical fluid anti-solvent, Biotech. Bioeng., 41 (1993), 341–346.

9 J.F. Brennecke and C.A. Eckert, Phase equilibria for supercritical fluid process design, AIChE J. 35 (1989) 1409–1427.

10 I.B. Petsche and P.G. Debenedetti, Solute-solvent interactions in infinitely dilute supercritical mixtures: a molecular dynamics investigation, J. Chem. Phys. 91 (1989) 7075–7084.

11 I.B. Petsche and P.G. Debenedetti, Influence of solute-solvent asymmetry upon the behavior of dilute supercritical mixtures, J. Phys. Chem. 95 (1991) 386–399.

12 P.G. Debenedetti and A. Chialvo, Solute-solute correlation in infinitely dilute supercritical mixtures, J. Chem. Phys. 97 (1992), 504–507.

13 A. Chialvo and P.G. Debenedetti, A molecular dynamics study of solute-solute microstructure in attractive and repulsive supercritical mixtures, Ind. Eng. Chem. Res. 31 (1992) 1391–1397.

14 B.L. Knutson, D.L. Tomaskó, C.A. Eckert, P.G. Debenedetti and A.A. Chialvo, A.A. Local density augmentation in supercritical solutions: a comparison between fluorescence spectroscopy and simulation results, in: F. Bright and M.E.P. MacNally (Eds.), Recent Advances in Supercritical Fluid Technology, Applications and Fundamental Studies, ACS Symp. Ser. 488, American Chemical Society, Washington DC, 1992, pp. 60–72.

15 R. Wu, L.L. Lee and H. Cochran, Structure of dilute supercritical solutions: clustering of solvent and solute molecules and the thermodynamic effects, Ind. Eng. Chem. Res. 29 (1990) 977–988.

16 S. Kim and K.P. Johnston, Clustering in supercritical fluid mixtures, AIChE J. 33 (1987) 1603–1611.

17 J.F. Brennecke, D.L. Tomasko, J. Peshkin and C.A. Eckert, Fluorescence spectroscopy studies of dilute supercritical solutions, Ind. Eng. Chem. Res. 29 (1990) 1682–1690.

18 J.F. Brennecke and C.A. Eckert, Fluorescence spectroscopy studies of intermolecular interactions in supercritical fluids, in: K.P. Johnston and J.M.L. Penninger (Eds.), Supercritical Fluid Science and Technology, ACS Symp. Ser. 406, American Chemical Society, Washington, DC 1989, pp. 14–26.

19 J.B. Hannay and J. Hogarth, On the solubility of solids in gases, Proc. R. Soc. London, 29 (1879) 324–326.

20 V. Krukonis, Supercritical fluid nucleation of difficult-to-comminute solids, AICHE Meeting, San Francisco, CA November 1984; paper 140 f.

21 J.W. Tom and P.G. Debenedetti, Particle formation with supercritical fluids: a review, J. Aerosol Sci., 22 (1991) 555–584.

22 P.M. Gallagher, V.J. Krukonis and L.J. VandeKieft, Gas anti-solvent recrystallization: application to the separation and subsequent processing of RDX and HMX, Proc. 2nd Int. Symp. Supercrit. Fluids., (1991) Boston, MA, pp. 45–48.

23 D.J. Dixon and K.P. Johnston, Molecular thermodynamics of solubilities in gas antisolvent crystallization, AIChE J. 37 (1991) 1441–1449.

24 C.J. Chang, A.D. Randolph and N.E. Craft, Separation of β-carotene mixtures precipitated from liquid solvents with high-pressure CO_2, Biotechnol. Prog. 7 (1991) 275–278.

25 C.J. Chang and A.D. Randolph, Precipitation of microsize organic particles from supercritical fluids, AIChE J. 35 (1989) 1876–1882.

26 D.W. Matson, R.C. Petersen and R.D. Smith, Formation of silica powders from the rapid expansion f supercritical solutions, Adv. Ceram. Mater. 1 (1986) 242–246.

27 D.W. Matson, R.C. Petersen and R.D. Smith, The preparation of polycarbosilane powders and fibers during rapid expansion of supercritical fluid solutions, Mater. Lett. 4 (1986) 429–432.

28 P.G. Debenedetti, J.W. Tom, X. Kwauk and S.D. Yeo, Rapid expansion of supercritical solutions: fundamentals and applications, Fluid Phase Equil., (1993), in press.

29 A.K. Lele and A.D. Shine, Dissolution and precipitation of polymers using a supercritical solvent, Polym. Prepr. (Am. Chem. Soc., Div. Polym. Chem.) 31(1) (1990) 677–678.

30 R.C. Petersen, D.W. Matson and R.D. Smith, Rapid precipitation of low vapor pressure solids from supercritical fluid solutions: the formation of thin films and powders, J. Am. Chem. Soc. 108 (1986) 2100–2102.

31 Boehringer Ingelheim, RESOMER Resorbable Polyesters, product literature, 1989.

32 K. Juni and M. Nakano, Poly(hydroxy acids) in drug delivery, CRC Crit. Rev. Ther. Drug Carrier Syst. 3 (1987) 209–232.
33 R. Mank and B. Thiele, Preparation of matrix tablet using polyglycolic acid, part 5, Pharmazie, 45(8) (1990), 594–595.
34 B.W. Mueller and W. Fischer, Manufacture of sterile sustained-release drug formulations using liquified gases, W. Germany Patent 3,744,329, July 6, 1989.
35 M. McHugh and V.J. Krukonis, Supercritical Fluid Extraction: Principles and Practice. Butterworths, Boston, 1986.
36 P.G. Debenedetti and S.K. Kumar, The molecular basis of temperature effects in supercritical extraction, AIChE J., 34 (1988) 645–657.